

Chapter 10

HARDWARE PLATFORMS FOR ELECTROSTATIC TUNING OF MEMS GYROSCOPE USING NATURE INSPIRED COMPUTATION

Didier Keymeulen¹, Michael I. Ferguson¹, Luke Breuer¹, Wolfgang Fink¹, Boris Oks¹, Chris Peay¹, Richard Terrile¹, Yen-Cheng², Dennis Kim², Eric MacDonald³, and David Foor⁴

¹ *Jet Propulsion Laboratory, MS 303-300, 4800 Oak Grove Dr., Pasadena, CA 91109, USA didier.keymeulen@jpl.nasa.gov;* ² *Mechanical and Aerospace Engineering Department, University of California, Los Angeles, CA 90095-1597;* ³ *University of Texas at El Paso, 500 West University dr., El Paso, TX, 79968-0523;* ⁴ *Texas A&M University-Kingsville, 700 University Blvd, Kingsville, TX, 78363*

Abstract: We propose a tuning method for Micro-Electro-Mechanical Systems (MEMS) gyroscopes based on evolutionary computation to increase the accuracy of MEMS gyroscopes through electrostatic tuning. The tuning method was tested for the second generation JPL/Boeing Post-resonator MEMS gyroscope using the measurement of the frequency response of the MEMS device in open-loop operation. We also report on the development and preliminary results of a hardware platform for integrated tuning based on “switched drive-angle” of MEMS gyroscopes whereby the same gyro is operated with its drive direction first at 0^0 and then at 90^0 . The control of this device is implemented through a digital design on a Field Programmable Gate Array (FPGA). The hardware platform easily transitions to an embedded solution that allows for the miniaturization of the system to a single chip.

Key words: MEMS, tuning, genetic algorithm, simulated annealing, FPGA

1. Introduction

Future NASA missions would benefit tremendously from an inexpensive, navigation grade, miniaturized inertial measurement unit (IMU), which surpasses the current state-of-the art in performance, compactness (both size and mass) and power efficiency. Towards this end, under current development at JPL's MEMS Technology Group are several different designs for environment tolerant [2], high performance, low mass and volume, low power MEMS gyroscopes. The accuracy with which the rate of rotation of micro-gyros can be determined depends crucially on the properties of the resonant structure. It is both difficult and expensive to attempt to achieve these desired characteristics in the fabrication process, especially in the case of small MEMS structures, and thus one has limited overall sensor performance due to unavoidable fabrication inaccuracies.

The accuracy with which a given vibratory gyroscope can determine the true inertial rate is crucially dependent on the properties of the two degree-of-freedom resonator. The problem with tracking orientation using only gyros is drift such as gyro bias which creates a steadily growing angular error, gyro white noise and gyro bias instability [11]. Today's commercial grade gyros (devices used in automobiles, camcorders) can only be used for a minute before the drift becomes distracting and the user needs to reset the orientation tracker. Tactile grade gyros used in short range missile guidance are good enough for head tracking for more than 20 minutes. Navigation grade gyros are required for space applications. Unfortunately, the price, weight and power ratio between navigation, tactile and commercial grade gyros follows the performance ratio. MEMS gyroscopes will be gradually closing in on the performance using techniques presented in the chapter.

One way to reduce the rate drift is to increase the sensitivity or scale factor relating volts out to radians per second of inertial input [3]. The scale factor is maximized when the resonant frequencies of the two modes of freedom of the MEMS gyroscope are identical. Symmetry of construction is necessary to attain this degeneracy. However, despite a symmetric design, perfect degeneracy is never attained in practice. Many methods have been developed for tuning MEMS post-resonator gyroscopes. For example [7] and [10] use adaptive and closed-loop methods, while [1] changes the frame of the pick-off signal. Our approach of gyro tuning is achieved through an electrostatic biasing approach [4]. This approach consists of applying bias voltages to built in tuning pads to electrostatically soften the mechanical springs. Because of the time consuming nature of the tuning process when performed manually, in practice any set of bias voltages that produce degeneracy is viewed as acceptable at the present time. Thus a need exists for reducing the time necessary for performing the tuning operation, and for

finding the optimally tuned configuration, which employs the minimal maximum tuning voltage.

This chapter describes the application of evolutionary computation to this optimization problem. Our open-loop and closed-loop methods used the following fitness function for each set of bias voltages applied to the built-in tuning pads: the frequency split between the two modes of resonance of the MEMS gyroscope. Our open-loop evaluation proceeds in two steps. First, it measures the open-loop frequency response using a dynamic signal analyzer. Second, it evaluates the frequency of resonance of both modes by fitting Lorentzian curves to the experimental data. The process of setting the bias voltages and the evaluation of the frequency split is completely computer automated. The computer controls a signal analyzer and programmable power supplies through General Purpose Interface Bus (GPIB). Our method has demonstrated that we can obtain a frequency split of 52mHz fully automatically in one hour compared with 200mHz obtained manually by humans in several hours.

The closed-loop method, also called “switched drive-angle” method, is based on controlling the gyro in a closed-loop along one axis and measuring the resonance frequencies along this axis at a given set of bias voltages, then swapping and driving the other axis, thereby extracting the resonant frequency of both axes. An evolutionary algorithm is then applied iteratively to modify the bias voltages until the resonant frequency of each axis is equal. A major advantage of this closed-loop approach is that the resonant frequencies can be extracted quickly (~1 second) as compared to the open-loop control system, which takes two orders of magnitude longer. The design of the closed-loop control approach is realized on an FPGA with augmented portability for future designs and implementations.

This chapter is organized such that Section 2 describes the mechanics of the MEMS micro-gyro, Section 3 describes the evolutionary computation applied to open-loop measurements of the resonance frequencies, Section 4 describes the closed-loop hardware platform and the results of our preliminary experiments, and Section 5 describes future directions and summarizes the project results.

2. Mechanism of the JPL MEMS Micro-gyroscope

The mechanical design of the JPL MEMS micro-gyro can be seen in Figure 1. The JPL/Boeing MEMS post resonator gyroscope (PRG), is a MEMS analogue to the classical Foucault pendulum. A pyrex post, anodically bonded to a silicon plate, is driven into a rocking mode along an

axis (labeled as X in Figure 1) by sinusoidal actuation via electrodes beneath the plate. In a rotating reference frame the post is coupled to the Coriolis force, which exerts a tangential “force” on the post. Another set of electrodes beneath the device senses this component of motion along an axis (labeled as Y in the figure) perpendicular to the driven motion. The voltage that is required to null out this motion is directly proportional to the rate of rotation to which the device is subjected and the voltage scale is reduced proportionally to the frequency split between the two modes of resonance. A change in capacitance occurs as the top plate vibrates due to the oscillating gap variation between this plate and the electrodes underneath. This change in capacitance generates a time varying sinusoidal charge that can be converted to a voltage using the relationship $V=Q/C$. The post can be driven around the drive axis by applying a time varying voltage signal to the drive petal electrodes labeled D1- (minus sign), D1+, D1in-, and D1in+ in Figure 1. Because there is symmetry in the device, either of the two axes can be designated as the drive axis. Each axis has a capacitive petal for sensing oscillations as well; driving axis: labeled S1+ and S1- in Figure 1, sensing axis: labeled S2+ and S2- in Figure 1. The micro-gyro has additional plates that allow for electrostatic softening of the silicon springs, labeled B1, BT1, B2, and BT2 in Figure 1. Static bias voltages can be used to modify the amount of softening for each oscillation mode. In an ideal, symmetric device, the resonant frequencies of both modes are equal; however, unavoidable manufacturing imperfections in the machining of the device can cause asymmetries in the silicon structure of the device, resulting in a frequency split between the resonant frequencies of these two modes. The frequency split reduces the voltage scale used to measure the rate of rotation to which the device is subjected, and thus the sensitivity for detection of rotation is decreased. By adjusting the static bias voltages on the capacitor plates, frequencies of resonance for both modes are modified to match each other; this is referred to as the tuning of the device using an electrostatic biasing approach [4].

In order to extract the resonant frequencies of the vibration modes, there are two general methods: 1) open-loop and 2) closed-loop control [3]. In an open-loop system, we are measuring the frequency response along the drive axis over a 50Hz band and extract from the measurement the frequency split. A faster method is a closed-loop control, whereby the gyro is given an impulse disturbance and is allowed to oscillate freely between the two resonance frequencies, using a hardware platform to control the switch of the drive-angles.

10. Hardware Platforms for Electrostatic Tuning of MEMS Gyroscopes using NATURE INSPIRED COMPUTATION

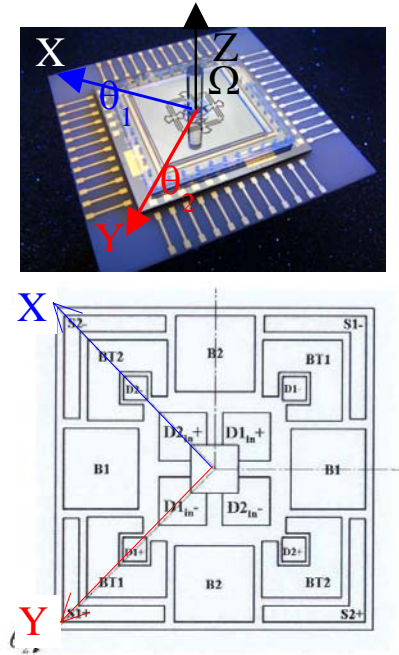


Figure 10-1. A magnified picture of the JPL MEMS micro-gyroscope with sense axis Y (S2-, S2+ electrodes used to sense, D2-, D2+, D2in- and D2in+ used to drive along the sense axis) and drive axis X (D1-, D1+, D1in-, and D1in+ used to drive, S1-, S1+ electrodes used to sense along the drive axis) and the electrodes used for biasing (B1, B2, BT1, BT2) (picture courtesy of C. Peay, JPL).

3. Evolutionary Computation using Open-Loop Measurement

3.1 Instrumentation Platform for Open-loop Frequency Response

The open-loop measurement consists of exciting the drive axis with a sine wave at a given frequency and measuring the resulting amplitude. This is done repeatedly throughout the frequency spectrum (frequency range from 3,300Hz to 3,350Hz; 50Hz span; 800 points,). Because of cross coupling between the different axes, two peaks in the amplitude response will appear at two different frequencies, showing the resonant frequencies of both axes

(Figure 4). This takes approximately 1.4 minutes to complete using our instrumentation platform (Figure 2) and must be repeated at least three times to average out noise.

The platform includes one GPIB programmable power supply for DC voltage, a GPIB signal analyzer to extract frequency responses (from 3.3kHz to 3.35kHz) of the gyro in open-loop, and a computer (PC) to control the instruments and to execute the evolutionary optimization algorithms. The power supply DC voltage controls the electrostatic bias voltages (connected to the plates B1, BT1, B2, and BT2 in Figure 1) that are used to modify the amount of damping to each oscillation mode. The GPIB signal analyzer generates a sine wave with a variable frequency (from 3300 Hz to 3350 Hz with a stepsize of 62.5 mHz – 800 points, 50Hz span) on the drive electrode (D1-, D1+, D1in-, and D1in+ in Figure 1) and measures the response signal on the sense electrode (S1-, S1+ in Figure 1) along the drive axis X.

A PC runs the instrument control tool, the measurement tool, and the evolutionary computation tool. The instrument control software sets up the static bias voltages using the GPIB power supply DC voltage and measures the frequency response along the X axis using the GPIB signal analyzer as shown in Figure 2. The software calculates the frequency split using peak fitting algorithms. Finally, the evolutionary computation software determines the new DC bias voltages from the frequency split. This procedure is repeated until a satisfactory (user defined) frequency split is obtained.

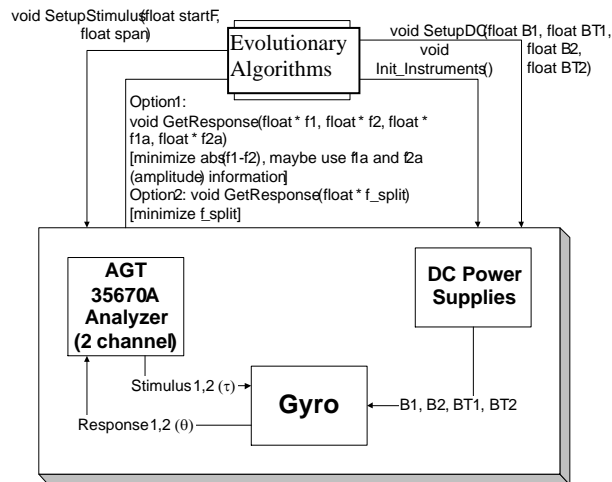


Figure 10-2. Software interface between the modified Simulated Annealing/modified Genetic Algorithm (Dynamic Hill Climbing) and the Instrumentation Platform using a GPIB programmable power supply DC voltage and a signal analyzer. The modified Simulated Annealing and the modified Genetic Algorithm are running on a PC, which controls the bias voltages and receives the frequencies of both resonance modes.]

3.2 Results of Evolutionary Computation

The MEMS post resonator micro-gyroscope is subject to an electrostatic fine tuning procedure, performed by hand, which is necessary due to unavoidable manufacturing inaccuracies. In order to fine tune the gyro, 4 bias voltages applied to 8 capacitor plates have to be determined within a range of -60V to $+15\text{V}$. The manual tuning took several hours and obtained a frequency split of 200 mHz.

In order to fully automate the time taking manual fine tuning process, we have established a hardware/software interface to the existing manual gyro-tuning hardware setup using commercial-off-the-shelf (COTS) components described in Section 3.1.

We developed and implemented two stochastic optimization techniques, for efficiently determining the optimal tuning voltages and incorporated them in the hardware/software interface: a modified simulated annealing related algorithm [9,6] and a modified genetic algorithm with limited evaluation (Dynamic Hill Climbing) [5,13]. These optimization techniques have also been used for other space applications [12].

3.2.1 Simulated Annealing Approach

We were able to successfully finetune both the MEMS post-resonator gyroscope and MEMS disk resonating gyroscope (a different gyro-design not discussed here) within one hour for the first time fully automatically. After only 49 iterations with the modified Simulated Annealing related optimization algorithm we obtained a frequency split of 125mHz within a 1V-discretization of the search space, starting with an initial split of 2.625Hz, using a 50Hz span and 800 points on the signal analyzer for the MEMS post-resonator gyroscope (Figure 3A). For the MEMS disk resonating gyroscope we obtained a frequency split of 250mHz/500mHz within a 0.1V-/0.01V-discretization of the search space, starting with an initial split of 16.125Hz/16.25Hz, after 249/12 iterations using a 200Hz span and 800 points on the signal analyzer (Figure 3B). All three results are better than what can be accomplished manually but worse than the results obtained by dynamic hill climbing (modified genetic algorithm). The reason for this is that instead of the peak fitting algorithm employed in the modified genetic algorithm approach a simplified, direct peak finding procedure was used in the Simulated Annealing approach.

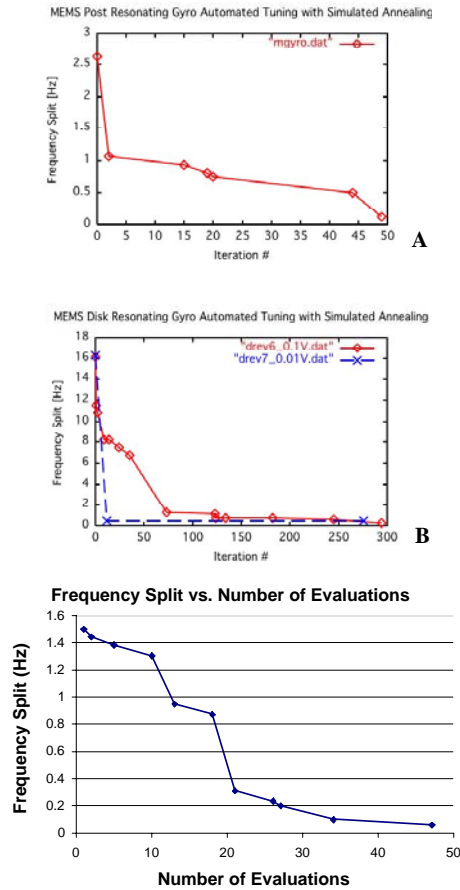


Figure 10-3. Frequency split as a function of number of evaluations: Simulated Annealing iterations: (A) for the MEMS post-resonator gyroscope; (B) for the MEMS disk-resonating gyroscope. (C) Dynamic Hill Climbing algorithm (modified genetic algorithm).

3.2.2 Genetic Related Algorithm Approach

We were also able to fine tune the MEMS post-resonator gyroscope within one hour fully automatically using a modified genetic algorithm: dynamic hill climbing. Figure 3 (C) shows the progress of the optimization algorithm aimed at minimizing the frequency split. Each evaluation is a proposed set of bias voltages. Our optimization method only needed 47 evaluations (51 min) to arrive at a set of bias voltages that produced a frequency split of less than 100mHz.

10. Hardware Platforms for Electrostatic Tuning of MEMS Gyroscope using NATURE INSPIRED COMPUTATION

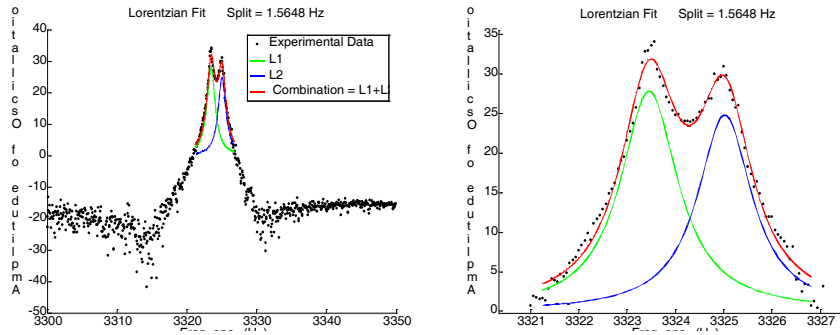


Figure 10-4. Frequency response (top: 50Hz band, bottom: 6Hz band) before tuning using the modified genetic algorithm. The frequency split is 1564.8mHz. The Y axis is measured in dB. The initial values of the four bias voltages are: B1 = 14.00V, BT1 = 14.00V, B2 = 14.00V, and BT2 = 14.00V. The right picture shows a zoomed in display of the frequency split over a 6Hz band.

Figures 4 and 5 show the frequency response for the unbiased micro-gyro respectively before and after tuning using the dynamic hill climbing and the peak fitting algorithm. After optimization of the bias voltages (Figure 5), the frequency split has been minimized to less than 100mHz and the two peaks are indistinguishable on an HP spectrum analyzer at 62.5mHz / division (50Hz span, 800 points) setting, which was used during the optimization process.

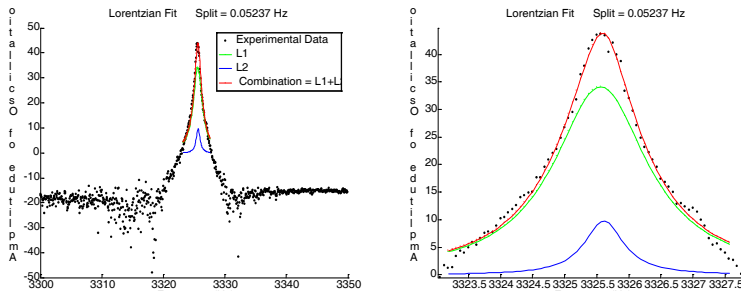


Figure 10-5. Frequency response (top: 50Hz band, bottom: 5Hz band) after tuning using the modified genetic algorithm. The Y axis is measured in dB. The tuning frequency split is 52mHz. The optimized values of the four bias voltages are: B1 = 4.00V, BT1 = 4.00V, B2 = 14.00V, and BT2 = -16.00V. The right picture shows a zoomed-in display of the frequency split over a 4Hz band.

The frequency split of 52mHz was verified using a higher resolution mode of the signal analyzer.

4. Hardware Platform using “switched drive-angle” Method

The principle of “switched drive-angle” electrostatic biasing is based on measuring the resonance frequencies of the drive axis at a given set of bias voltages then swapping and driving the other axis, thereby extracting the resonant frequencies of both axes. An algorithm is then applied iteratively to modify the bias voltages until the resonant frequency of each axis is equal. A major advantage of this closed-loop approach is that the resonant frequencies can be extracted quickly (~1 second) as compared to the open-loop control system, which takes two orders of magnitude longer. The design of the electrostatic biasing approach is realized on an FPGA with augmented portability for future designs and implementations.

4.1 Control of the MEMS Micro-gyro

The “switched drive-angle” approach requires a closed-loop control whereby the gyro is given an impulse disturbance and is allowed to oscillate freely. This so called “pinging” of the vibration mode allows the gyroscope to immediately settle to its natural frequency. The corresponding frequency, F_1 , is measured from the sensing plate under the drive axis X. Because the device is relatively symmetric, the drive and sense axes are swapped and the other mode is pinged to get F_2 . The difference in the frequencies, i.e., frequency split, is determined very quickly using this technique, about 1.5 seconds, roughly 50 times faster than from the open-loop control method. This ability to quickly swap the drive axis with the sense axis is a feature of our FPGA Gyro Digital System (GDS).

The circuitry of the closed-loop control system includes a drive loop and a sense rebalance loop [1]. The drive loop takes the input from the “drive sense” petal (S1-, S1+ electrodes along the drive axis), and outputs the forcing signal to the “drive-drive” petal electrodes (D1-, D1+, D1in- and D1in+ electrodes along the drive axis). The sense rebalance loop receives input from the “sense-sense” petal (S2-, S2+ electrodes along the sense axis), and forces or rebalances the oscillations back along the drive axis with a forcing signal to the “sense drive” (D2-, D2+, D2in- and D2in+ electrodes). The magnitude of this forcing function in the rebalance loop is related to the angular rate of rotation. The closed-loop control has also several scaling coefficients, denoted as K_i , which allow for a mixing of the sensed signals from both axes and a swapping of the drive- and sense-axis, thus permitting the tuning algorithm to measure the resonance frequency along the X- or Y-axis, or, indeed, any axis between X and Y [3].

The drive loop implements an Automatic Gain Control (AGC) loop combined with finite impulse response (FIR) filters. Because the amplitude of the freely oscillating drive axis will naturally decay, the AGC is implemented in a way to lightly drive or damp, depending on the circumstance, the drive axis so that the amplitude of the driven signal is constant and the gyroscope is maintained in an oscillation mode at the natural frequency. The optimal parameters of the FIR filters and the AGC loop to maintain the oscillation of the gyroscope have been determined by the UCLA team using a DSP measurement system and a UCLA MatLab modeling tool [8].

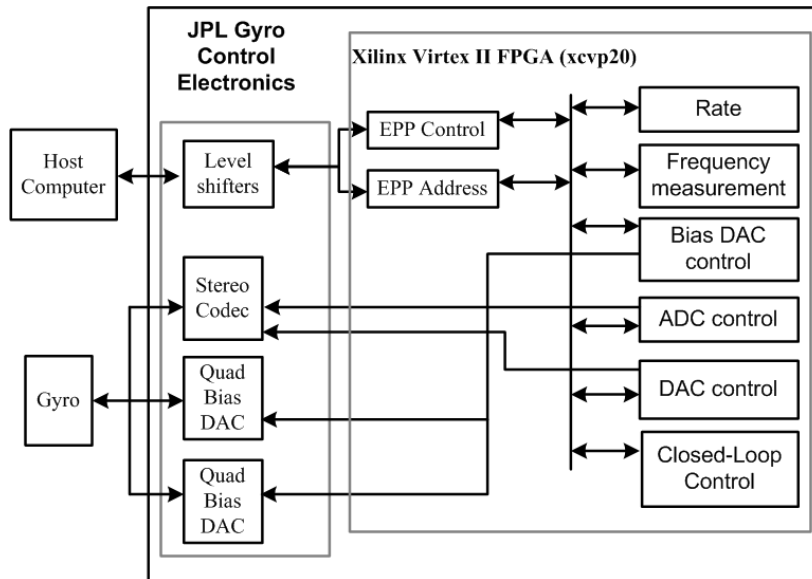


Figure 10-6. Block diagram of the entire closed-loop control system.

4.2 Gyro Digital System (GDS)

The system used to implement the control, operation, and observability of the micro-gyro is referred to as the Gyro Digital System (GDS). Figure 6 illustrates the implementation of the analog and digital systems used to control the micro-gyro. The key circuit elements that allow proper operation of the micro-gyro include the audio codec (Stereo Digital to Analog Converter DAC), high voltage Analog to Digital Converters (ADCs), IEEE-1294 Enhanced Parallel Port (EPP) interface replaced by a UART interface,

frequency measurement and the Digital Signal Processor (DSP) functionality integrated into a Xilinx Virtex II FPGA.

The audio codec is used to translate the analog sensing signals for both the drive and the sense axes. Its stereo capabilities allow for two inputs and two outputs. The high-voltage DACs are utilized for the setting of the electrostatic bias voltages on the gyroscope, which range from +15V to -60V. The parallel port interface allows for user input/output capabilities. The user can configure the coefficients for the finite impulse response (FIR) filters along with the scaling coefficients (K1 through K8) and automatic gain control (AGC) proportional integral (PI) coefficients (Kp and Ki). The codec is configured through this interface as well.

4.3 Results

Using this FPGA digital control system, the micro-gyro was operated for a period of several hours and provided a frequency measurement that was stable to 1 mHz.

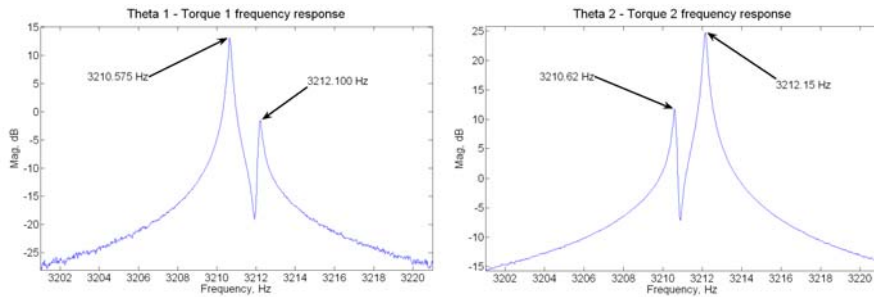


Figure 10-7. Bode magnitude of the experimental frequency response data for a non-tuned MEMS micro-gyroscope ($B_1=B_2=BT_1=BT_2=14V$). Left drive axis on the axis X. Right drive axis on the axis Y

This FPGA system has not yet been tested in the mode where the drive- and sense-axes are swapped, but we have performed experiments using a DSP platform controlled by a Simulink environment running on a PC that demonstrates the feasibility of the closed-loop approach. In Figure 7 we show the frequency response of a non-tuned MEMS gyroscope ($B_1=B_2=BT_1=BT_2=14V$) with two peaks for each of the resonance frequencies when drive axis is along axis X (Left) and when drive axis is along axis Y (Right). Using a closed-loop control, the UCLA team was able to find the correct AGC and FIR filter parameters to maintain the gyro in an oscillating mode at the natural frequency. The DSP platform measured the

10. Hardware Platforms for Electrostatic Tuning of MEMS Gyroscope using NATURE INSPIRED COMPUTATION

frequency of both modes by swapping the drive and sense axis ($F_1=3210.62\text{Hz}$ and $F_2=3212.15\text{Hz}$) as shown on Figure 7. Keeping the value of the AGC and FIR parameters constant and changing the value of the DC bias voltage, we were able to maintain the gyro in an oscillation mode and to extract both resonance frequencies, which have changed due to the update DC bias voltage.

The next step is to couple the FPGA frequency measurement with the genetic algorithm and the simulated annealing running on the PC. The ultimate goal is to implement the GA and the SA on a microprocessor integrated into a FPGA.

5. Conclusion

The tuning method for MEMS micro-gyroscopes based on evolutionary computation shows great promise as a technology to replace the cumbersome, manual tuning process. We demonstrated, using an open-loop measurement that we can, for the first time fully automatically, obtain a four times smaller frequency split at a tenth of the time, compared to human performance. We also showed that the “switched drive-angle” system has the option of swapping the drive- and sense-axes, thus decreasing the time required for tuning by more than a factor of fifty compared to the open-loop approach. Additionally, a future design will include a microprocessor on-chip to allow for in-situ re-tuning of the MEMS micro-gyroscope if there is an unexpected change in the behavior due to radiation, temperature shift, or other faults.

The novel capability of fully automated gyro tuning, integrated in a single device next to the gyro, enables robust, low mass and low power high-precision Inertial Measurement Unit (IMU) systems to calibrate themselves autonomously during ongoing missions, e.g., Mars Ascent Vehicle.

Acknowledgements

The work described in this publication was carried out at the Jet Propulsion Laboratory, California Institute of Technology, under a contract with the National Aeronautics and Space Administration. Special thanks to Tom Prince, who has supported this research through the Research and Technology Development grant entitled “Evolutionary Computation Technologies for Space Systems”.

References

1. Y. Chen, R. M'Closkey, T. Tran and B. Blaes. "A control and signal processing integrated circuit for the JPL-Boeing micromachined gyroscopes" (submitted to IEEE)
2. M. I. Ferguson, D. Keymeulen, C. Peay, K. Yee, D. Li, "Effect of Temperature on MEMS Vibratory Rate Gyroscope", in Proceedings of the IEEE Aerospace Conference, Big Sky, March 2005.
3. K. Hayworth, "Continuous Tuning and Calibration of Vibratory Gyroscopes", In NASA Tech Brief, Oct 2003 (NPO-30449)
4. K. Hayworth, K. Shcheglov, T. Humphreys, A. Challoner, "Electrostatic Spring Softening in Redundant Degree of Freedom resonators", patent US 6,823,734 B1, JPL and Boeing, Nov. 30, 2004.
5. J.H. Holland, *Adaptation in Natural and Artificial Systems*, The University of Michigan Press, Ann Arbor, Michigan, 1975.
6. S. Kirkpatrick, C.D. Gelat, M.P. Vecchi,, "Optimization by Simulated Annealing," *Science*, 220, 671--680, 1983.
7. Leland, R.P., "Adaptive mode tuning vibrational gyroscopes", *IEEE Trans. Control Systems Tech.*, vol. 11, no. 2, pp242-247, March 2003.
8. R. M'Closkey and D. Kim, "Real-time tuning of JPL-Boeing MEMS gyro", personal communication, JPL, March 2005.
9. N. Metropolis, A.W. Rosenbluth, M.N. Rosenbluth, A.H. Teller, E. Teller, "Equation of State Calculation by Fast Computing Machines," *J. of Chem. Phys.*, 21, 1087--1091, 1953.
10. Painer C.C., Shkel A.M., "Active structural error suppression in MEMS vibratory rate inte-grating gyroscopes", *IEEE Sensors Journal*, vol.3, no.5, pp. 595-606, Oct. 2003.
11. Ed. Kay Stanney, "Handbook of Virtual Environment Technology", Lawrence Erlbaum Associates, 2002.
12. R. J. Terrile, et al., "Evolutionary Computation Technologies for Space Systems", in Proceedings of the IEEE Aerospace Conference, Big Sky, March 2005
13. D. Yuret, M. de la Maza, "Dynamic Hill Climbing – Overcoming limitations of optimization techniques", AI Laboratory, MIT, Cambridge, MA 02139, USA